Journal of Catalysis 458 (2026) 116860

Contents lists available at ScienceDirect

Journal of Catalysis

journal homepage: www.elsevier.com/locate/jcat

One-pot stepwise and consecutive mechanistically incompatible solvent-free reactions: Synthetic and mechanistic insights☆

Jorge Cambronero-Arregui [a], Alejandro V. Martínez [b], Elisabet Pires [a], José A. Mayoral [a], Alejandro Leal-Duaso [a,*]

[a] Instituto de Síntesis Química y Catálisis Homogénea (ISQCH), CSIC-Universidad de Zaragoza, Faculty of Science, calle Pedro Cerbuna 12, E-50009 Zaragoza, Spain
[b] Asociación de la Industria Navarra (AIN), Carretera Pamplona 1, Edificio AIN, E-31191 Cordovilla, Pamplona, Spain

ARTICLE INFO

Keywords:
One-pot
Coupling
Hydrogenation
Palladium
Release-and-capture
Nabumetone
Resveratrol

ABSTRACT

Pd nanoparticles supported on an accessible laponite clay are efficient and highly recoverable catalytic systems in benchmark coupling and hydrogenation reactions under solvent-free conditions. In this paper, we explore the use of these supported catalytic systems in one-pot stepwise and consecutive reactions with excellent isolated yields. Whereas the catalyst recovered from hydrogenation reactions remains active in both coupling and hydrogenation processes, the catalyst used in coupling reactions is progressively deactivated for further hydrogenations. This behavior is not due neither to the nanoparticles agglomeration nor to Pd leaching, but to the formation of Pd(II) on the catalyst surface, disclosing a clear XPS evidence for the theory of the "release and capture" mechanism. Nonetheless, the hydrogenation activity is fully recovered after reducing this surface Pd(II) using ethanol. Finally, we have applied this strategy in the synthesis of products with practical pharmaceutical interest such as nabumetone and resveratrol.

1. Introduction

Palladium nanoparticles (Pd NPs) are consolidated nanocatalysts for efficient and selective catalytic processes [1,2]. Indeed, the unique structured surface capacity and electronic properties of Pd makes it highly suitable for bottom-up synthesis of nanoparticles [3,4]. This type of synthetic methodology allows to guarantee the size and chemical composition of the nanoparticles [5,6], thus influencing their resulting catalytic activity. However, non-stabilized metal nanoparticles present agglomeration over time that reduce their specific surface area. Various organic ligands, polymers, and surfactants have been used for stabilization of nanoparticles through steric, electronic, and electrosteric repulsion forces [7,8]. After preparation, nanoparticles are usually supported over solid materials [9]. This immobilization increases the stability of nanoparticles and, above all, allows their recovery and reuse in order to design recoverable heterogeneous catalytic systems [10]. Natural and synthetic clays, such as laponite, zeolites, oxides, organic polymers, and carbonaceous materials are typical solid supports used for metal nanoparticles [4,11,12].

Among the different palladium-catalyzed reactions, C–C coupling and hydrogenation reactions stand out due to the industrial relevance of these processes. Cross-coupling reactions provide synthetic access to a large variety of value-added chemicals minimizing the waste generation [13,14], while metal-catalyzed hydrogenation of organic unsaturated compounds is widely applied in industrial processes, from petrochemistry to the synthesis of fine-chemicals and fertilizers, or to the remediation of organic pollutants [15–17]. These processes are highly efficient due to the use of transition metal catalysts, as well as sustainable, thanks to the total atom economy and low waste generation of hydrogenation reactions [18]. In fact, the hydrogenation of unsaturated compounds represents over 5% of total reactions carried out in the pharmaceutical industry [19]. Both homogeneous and heterogeneous catalysts have been applied to promote hydrogenation reactions [18]. However, heterogeneous catalysts are by far the most widely used in industrial hydrogenations [20]. Among the transition metals, palladium leads to efficient hydrogenation catalysts that allow for the use of more moderate pressure and temperature conditions [21–23]. When using nanoparticles, hydrogenation takes place on the surface of the nanoparticle, without the participation of species leached from the nanoparticles [24]. As a result, catalytic hydrogenations are strongly

☆ †Dedicated to the 70th anniversary of Professor Víctor Martínez-Merino.

* Corresponding author.
E-mail address: alduaso@unizar.es (A. Leal-Duaso).

https://doi.org/10.1016/j.jcat.2026.116860
Received 5 February 2026; Received in revised form 26 March 2026; Accepted 26 March 2026
Available online 30 March 2026

influenced by the size and shape of nanoparticles [25,26]. In this context, interesting examples of size-dependent catalytic hydrogenation reactions have been recently described using precisely controlled Pd nanoclusters [27–29].

In diverse industrial and pharmaceutical processes, an organic reaction step is followed by the hydrogenation of the first reaction product [30]. Therefore, the development of scalable one-pot and consecutive catalyzed processes continues to attract increasing interest [31–33]. It is possible to find examples such as Heck plus Suzuki-Miyaura tandem and domino processes [34,35], Mizoroki-Heck cascade reactions [36], Heck reactions coupled to C–H activations [37,38] or carbonylations [39,40], as well as some recent examples of tandem processes, such as asymmetric transfer hydrogenation followed by Sonogashira coupling [41], and Suzuki-Miyaura coupled with hydrogenation [42,43].

Surprisingly, there are only a few examples dealing with the combination of Mizoroki-Heck with hydrogenation [44], even at a compact reactor scale [45]. The catalyst consisted on homogeneous $Pd(AcO)_2$, 5% Pd/C or, as described by Climent et al. supported Pd for the coupling of 4-methoxyiodoanisole and methyl vinyl ketone followed by hydrogenation [45–49]. Different solids, including magnesium oxide, hydrotalcites, hydroxyapatite, aluminium oxide (γ-Al_2O_3), and titanium dioxide (TiO_2), were studied for supporting this Pd catalyst. Therefore, in these works, both homogeneous Pd complexes and heterogeneous supported Pd catalysts, without a real control in the size and surface characteristics of the catalyst, have been applied in one-pot processes based on C–C coupling plus hydrogenation. However, to the best of our knowledge, nanoparticulate catalysts have not yet been studied, which is rather surprising given the high catalytic activity of Pd nanoparticles to promote both reactions.

In this line, it is particularly important to design recoverable catalytic systems able to sequentially promote all reaction steps. In fact, the combination of reactions promoted by the same type or compatible catalyst is well known, however, the use of a priori non compatible catalysts is scarce. In this regard our group described some years ago the use of solids basic and acid catalysts in one-pot reactions, based on the concept of isolated catalytic sites [50].

Here we explore the possibility of using the same catalytic sites to combine reactions that occur through different mechanisms. Some years ago, we described the most recoverable catalyst for the Mizoroki-Heck reaction [10]. Therefore, in this work we have tested whether this type of supported nanoparticulate catalyst is active and recoverable in hydrogenation reactions. As it has been the case, we have tested the same catalyst in benchmark cross-coupling plus hydrogenation both one-pot stepwise and consecutive reactions, showing whether the catalyst used in one reaction could be reused in the other one, despite their different—a priori incompatible—catalytic mechanisms. Thus, we present stable, active, recoverable, and affordable catalytic systems based on clay-supported palladium nanoparticles to promote coupled C–C coupling plus hydrogenation reactions, for the first time. Furthermore, the results obtained provide valuable mechanistic insights.

2. Results and discussion

2.1. Preparation and characteristics of the catalytic systems

Designer heterogeneous catalytic systems were prepared by supporting palladium nanoparticles on laponite®. Laponite® is a white synthetic smectite clay, *i.e.* an affordable layer-type hydrous magnesium silicate with reproducible textural properties and composition, with empirical formula: $Na_{0.7}[(Si_8Mg_{5.5}Li_{0.3})O_{20}(OH)_4]$. First, PVP-stabilized Pd nanoparticles were straightforwardly prepared in ethanol using Pd (II) chloride as a metallic precursor [6,10]. Then, this nanoparticle suspension was dispersed on laponite®, and the remaining ethanol was evaporated under vacuum, leading to a free-flowing powder. The use of PVP was proven to be essential to prevent the almost complete agglomeration of black palladium (Fig. S-102), and thus to guarantee both the stability and recyclability of the resulting heterogeneous catalysts (Tables S-10–S-12).

The Scanning Electron Microscopy (FESEM) analyses of the as-prepared catalytic system, and especially its TEM micrographs (Fig. S-91), reveal a quite homogeneous distribution of spherical nanoparticles along the clay structure. As it can be seen in the TEM analysis from Fig. 1, the sizes range of the supported Pd NPs was quite large (from 1 to 17 nm), with a mean size of 4.7 ± 3.6 nm. Powder X-Ray Diffraction (PXRD) analysis of the solid catalyst shows the main crystallographic diffraction planes of crystalline palladium, fitting the experimental data to a face centered cubic structure for the Pd nanoparticles. When comparing elemental and ICP-AES analyses, both techniques showed a consistent palladium content. Finally, the specific surface area (301.9 $m^2\ g^{-1}$) and related parameters (pore volume of 0.264 $cm^3\ g^{-1}$ and pore diameter of 3.50 nm) determined by N_2 adsorption by applying the BET theory to the heterogeneous catalyst (Table S-4) are similar to those of the laponite® support (Table S-3).

2.2. First step: C–C coupling reaction

The supported Pd nanoparticle catalytic systems described before were first used in several benchmark C–C Heck-Mizoroki coupling reactions, in the presence of triethylamine as a base (Scheme 1). These Pd-catalyzed reactions yielded excellent conversions and selectivities to higher-value products such as *n*-butyl cinnamate (**1**) and different *(E)*-stilbenes (**2–4**).

Then, the PVP-Pd NPs/laponite® catalytic system was applied to the synthesis of resveratrol, used as both anti-inflammatory drug and antifungal additive. First, one of the products described in Scheme 1, *(E)*-1,3-dimethoxy-5-(4-methoxystyryl)benzene (**5**), is a direct precursor of resveratrol that was obtained by coupling 1-iodo-3,5-dimethoxybenzene and 4-methoxystyrene. Deprotection of the three methoxy groups of **5** (see the Supplementary Information for additional details) led to resveratrol with an isolated yield of 92%.

Given the practical interest of this reaction, we studied the recovery of the catalyst in the synthesis of **5**, results are gathered in Table S-2. In this case, the catalytic system was recovered and reused up to 10 reaction cycles without any sign of catalytic deactivation (observing quantitative conversions and isolated yields of 89–99%). This represents an accumulated TON value of 952 for the synthesis of the resveratrol precursor.

It is interesting to highlight the notable stability (under air and versus Pd agglomeration) and recyclability of the catalytic system PVP-Pd NPs/laponite®. For example, in the case of the benchmark coupling reaction for the synthesis of *n*-butyl cinnamate (**1**), over 50 reaction cycles were promoted without any catalytic deactivation, which makes it easy to achieve outstanding catalytic productivity values, such as an accumulated TON greater than 5000.

2.3. Second step: hydrogenation reaction and tandem hydrogenation processes

Secondly, the designed catalytic systems based on PVP-Pd NPs/laponite® were applied, for the first time, in the catalytic hydrogenation of different interesting compounds in the absence of any solvent. The experimental parameters were optimized for the benchmark catalytic hydrogenation of the substrates prepared previously by Heck-Mizoroki coupling reactions, namely *(E)*-butyl cinnamate (**1**) and *(E)*-stilbene (**2**) (Scheme 2).

The influence of the catalyst amount, hydrogen pressure, temperature, and reaction time was studied. At the end of the reaction, the hydrogenated product was extracted with an organic solvent and analyzed by gas chromatography, prior to the determination of substrate conversion and product yield.

Both *(E)*-butyl cinnamate (**1**) and a series of differently substituted (*E*)-stilbenes (**2–5**) were completely hydrogenated over the supported

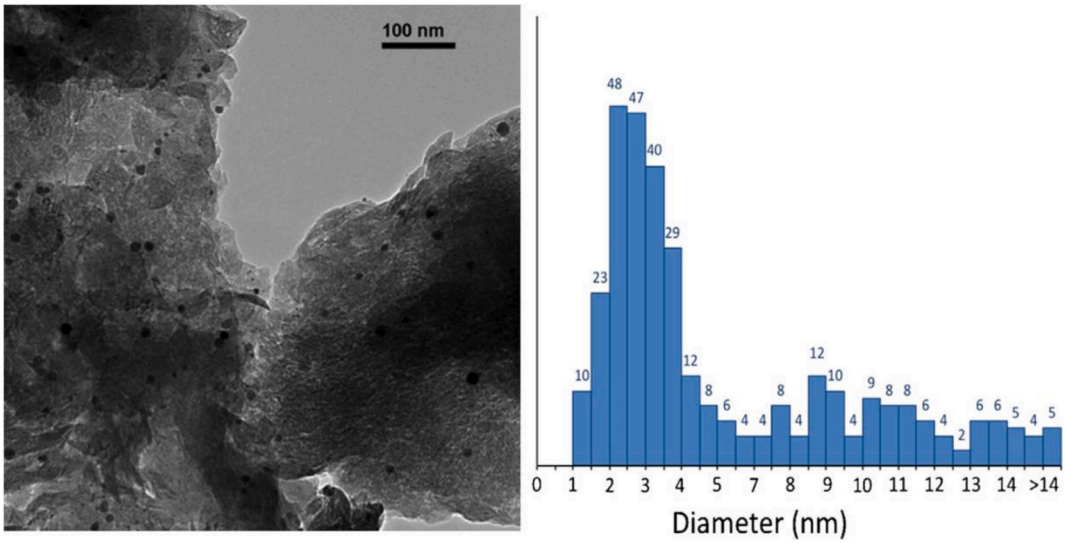

Fig. 1. TEM micrograph and size distribution of PVP-Pd NPs/laponite® system.

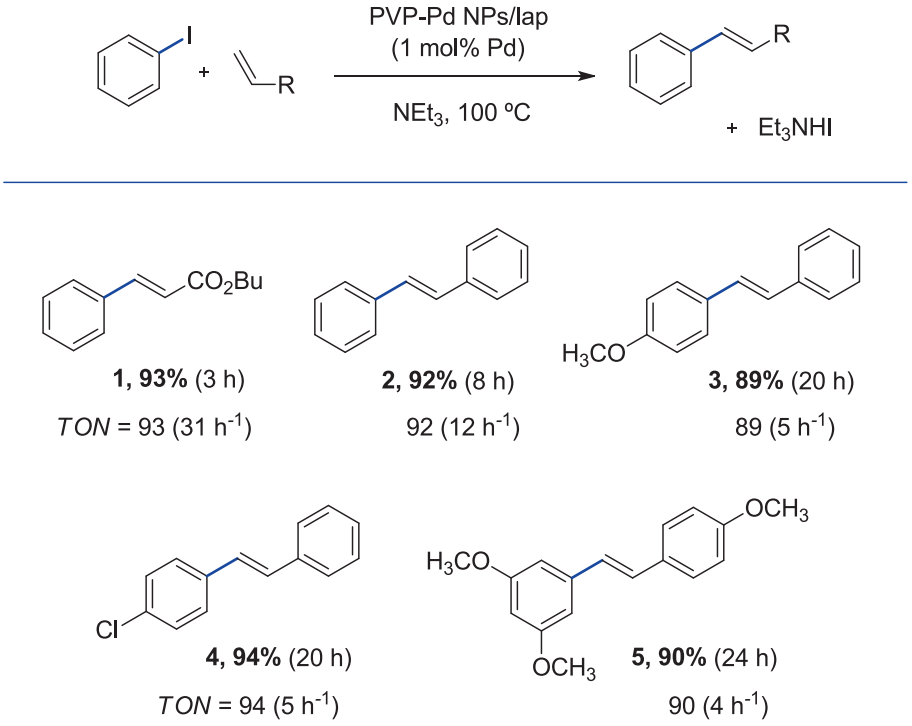

Scheme 1. Isolated yields and catalytic parameters (TON and TOF in h^{-1}) in Heck-Mizoroki coupling reactions catalyzed by the PVP-Pd NPs/laponite® system.

palladium (1 mol%) catalyst using 1 bar of H_2, in the absence of any additional solvent (Table 1). Moreover, in the case of *(E)*-butyl cinnamate (**1**), quantitative conversion of the olefin to *n*-butyl 3-phenylpropanoate was achieved in less than 10 min at 80 °C, which means a TOF of 558 h^{-1}.

It is interesting to note that, in spite of the fact that the hydrogenation of the double bond in (*E*)-stilbenes (**2–5**) is more difficult than in the case of more activated *(E)*-butyl cinnamate (**1**), quantitative results were obtained in both cases under similar reaction conditions, although in slightly longer reaction times (from 15 to 30 min, see Table 1, entries 2–4). The hydrogenation of stilbenes presenting substitution with both electron donor groups (such as the methoxy substituent in **3** and **5**) and electron withdrawing groups (such as the chlorine in **4**) was achieved under similar conditions. Moreover, the ester group in substrate **1** was not reduced under these hydrogenation conditions, leading to the selective hydrogenation of conjugated olefins.

Once the reaction conditions were optimized, the PVP-Pd NPs/laponite® systems were applied to promote the hydrogenation of a scope of substrates (Table 1). All of the substrates studied were completely hydrogenated in less than 45 min.

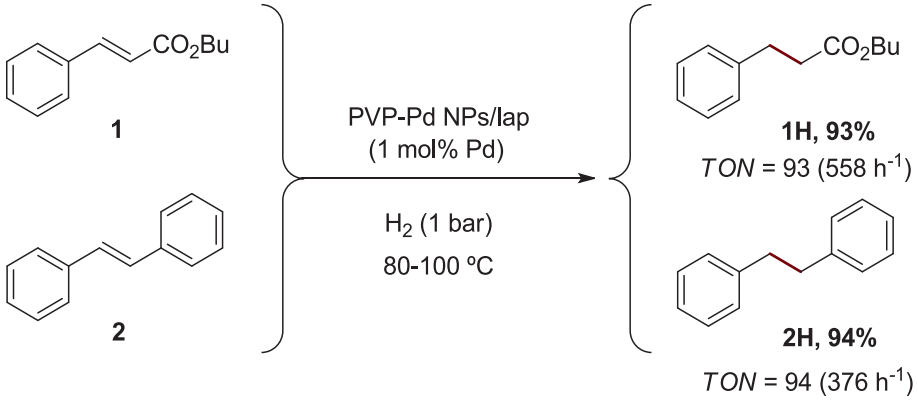

Scheme 2. Hydrogenation reactions of *(E)*-butyl cinnamate and *(E)*-stilbene catalyzed by the PVP-Pd NPs/laponite® system.

Table 1
Substrates scope in hydrogenation reactions catalyzed by PVP-Pd NPs/laponite®.

Entry [a]	Substrate	Product	Time (min)	Conv. (%) [b]	Isolated yield (%)[b]	TOF (h^{-1})
1	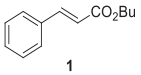 1	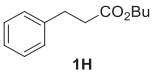 1H	10	100[c]	93	558
2	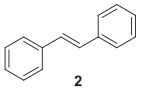 2	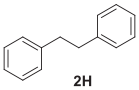 2H	15	100[c]	94	376
3	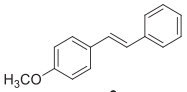 3	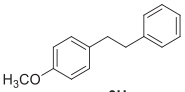 3H	30	100	94	188
4	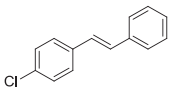 4	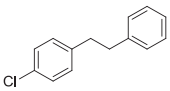 4H	30	100	96	192
5	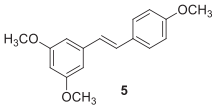 5	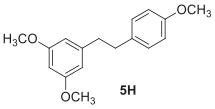 5H	45	100	91	121
6	 6	 6H	40	100	79	119
7	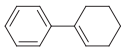 7	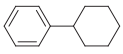 7H	20	100	91	273
8	 8	 8H	30	100	84	168
9	 9	 9H	30	100	87	174

[a] Reaction conditions: The substrate (0.3 mmol) was adsorbed onto the solid PVP-Pd NPs/laponite® (1 mol% Pd) in an autoclave vessel. Then, the vessel was placed under vacuum prior to its filling with H_2 (1 bar), sealed, and heated at 100 °C. Reaction crudes were extracted using *n*-hexane. [b] Conversion and selectivity were determined by GC and ^{1}H NMR. [c] Hydrogenation of *n*-butyl cinnamate and *(E)*-stilbene were completed at 80 °C.

As shown in Table 1, the catalytic system was also tested in the hydrogenation of different substrates. 2-Vinylpyridine (**6**) was converted to 2-ethylpyridine (**6H**), without observing any poisoning effect of pyridine. Also, a poorly-activated trisubstituted alkene, namely 1-phenyl-1-cyclohexene (**7**) was quantitatively hydrogenated to 1-cyclohexylbenzene (**7H**), a cyclic diene such as *cis,cis*-1,3-cyclooctadiene (**8**) to cyclooctane (**8H**), and, finally, the nitro group of nitrobenzene (**9**) to the amine in aniline (**9H**). In all cases, the conversion was complete, with high isolated yields of the desired products. Thus, the designed catalyst allows for the selective hydrogenation of

mono-, di-, and trisubstituted olefins, together with conjugated double bonds, and specific functional groups such as nitro ones.

As can be seen in the error bar experiments summarized in Fig. S-101, the reproducibility in the results presented for the different reactions studied in this work (by 5 times) is ensured (≤±1% for hydrogenations and ±2–3% for coupling and one-pot reactions).

In general, catalysts are recovered and reused for the hydrogenation of the same substrate. However, electronic properties of different substrates can affect the catalyst recyclability, therefore, we decided to evaluate the catalytic activity of the reused PVP-Pd NPs/laponite® system by consecutively hydrogenating a series of eight different substrates. The chosen approach in this case was a one-pot process, which means that no purification of the reaction product was necessary prior to carrying out the following hydrogenation. Then, after each reaction, the catalyst was washed, dried, and reused in consecutive hydrogenation reactions (Table 2). In all cases (for each substrate), results were similar to those obtained with the fresh catalyst (see Table 1).

As shown in Table 2, the recovered catalytic system was able to hydrogenate all different substrates without any loss of catalytic activity. Then, the PVP-Pd NPs/laponite® catalyst recovered after promoting 8 catalytic cycles was characterized by electron microscopy. FESEM microscopy reveals a noticeable decrease of the size of clay particles after the last reaction cycle, due to the delamination of the support during catalysis (Fig. 2a). On the other hand, the TEM micrographs show a high number of palladium nanoparticles that maintain an average size similar to those of the original solid catalyst (Fig. 2b). This indicates that the mean nanoparticle size is maintained during hydrogenation reactions, suggesting a heterogeneous hydrogenation mechanism without major surface modifications [18]. Moreover, the elemental analysis of the used solid provided a constant Pd content, which, together with the ICP analyses of the extraction supernatants, revealed that palladium was not significantly leached during hydrogenation reactions (Table S-9).

2.4. Pd-catalyzed one-pot and sequential reactions and mechanistic insights

Given the high efficiency and recoverability of the PVP-Pd NPs/laponite® system for both coupling and hydrogenation reactions, we proposed to test the use of these heterogeneous catalysts to consecutively promote coupled reactions based on Mizoroki-Heck plus hydrogenation. However, the same catalyst is able to promote coupling and hydrogenation of the alkenes used as reagents, so both processes cannot be simultaneously performed. Thus, we carried out a one-pot stepwise approach without purification of any intermediate (Scheme 3). After coupling iodobenzene with either *n*-butyl acrylate or *(E)*-styrene under the optimized conditions, the resulting coupled aryl alkenes were hydrogenated with H_2 (1 bar) at 80 °C, and the final reaction products were extracted and analyzed as previously described.

As it can be seen in Table 3, the designed catalytic system was capable of completely promoting the Heck-Mizoroki coupling plus hydrogenation coupled reactions, providing 90% of overall isolated yield for substrates **1** and **2** (entries 1 and 4). Both multi-step approaches are possible with similar results, i.e. the direct one-pot stepwise process without purification of the Heck-Mizoroki product and the sequential process consisting of two consecutive reaction steps with isolation and purification of the first reaction product. However, upon recovery of the catalyst it can be seen that, although the catalyst is still active for promoting any coupling reaction after the hydrogenation step (with similar isolated yields, entries 2, 3, 5, and 6), it is deactivated for further hydrogenation reactions.

Table 2
Catalyst recovery study of the PVP-Pd NPs/laponite® system in the consecutive one-pot hydrogenation of different substrates.

Entry [a]	Cycle	Substrate	Conv. (%) [b]	Isolated yield (%) [b]	TOF (h^{-1})
1	1	**1** 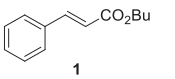	100	93	558
2	2	**2** 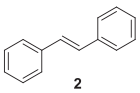	100	94	188
3	3	**3** 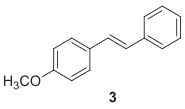	100	94	188
4	4	**4** 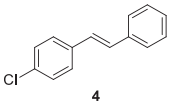	100	96	192
5	5	**6** 	100	79	119
6	6	**7** 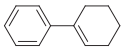	100	91	273
7	7	**8** 	100	84	168
8	8	**9** 	100	87	174

[a] Reaction conditions: The substrate (0.3 mmol) was adsorbed onto PVP-Pd NPs/laponite® (1 mol% Pd) in an autoclave vessel. Then, the vessel was placed under vacuum prior to its filling with H_2 (1 bar), sealed, and heated at 80/100 °C for the corresponding time. The system was dried between each cycle. [b] Conversion and selectivity were determined by ^{1}H NMR.

The TEM analysis of the solid catalyst after the one-pot reaction shows the presence of a number of palladium nanoparticles with a dispersion of sizes similar to the fresh catalyst (Fig. 3b). Moreover, the ICP-OES analysis of both the used catalytic systems and the extraction supernatants indicate low leaching of palladium during the catalysis (<0.5% per one-pot cycle, mostly coming from the coupling reaction as seen above, see Tables S-8 and S-9). Both results seem to justify the high activity of the recovered catalyst in subsequent coupling reactions.

On the other hand, it is interesting to note that triethylammonium iodide salt, the concomitant byproduct of the Mizoroki-Heck coupling reaction, is accumulated after each cycle over the laponite® surface and thus could poison the catalyst after reuse [6,10]. In spite of identifying the presence of this salt in the FESEM micrographs, as an organic layer covering the clay, and in the EDX analyses (Fig. 3a and c), no catalyst deactivation was observed after catalyzing several coupling reactions. However, it can be speculated that this organic salt could block the access of hydrogen to the catalyst surface, thus preventing the catalyst to

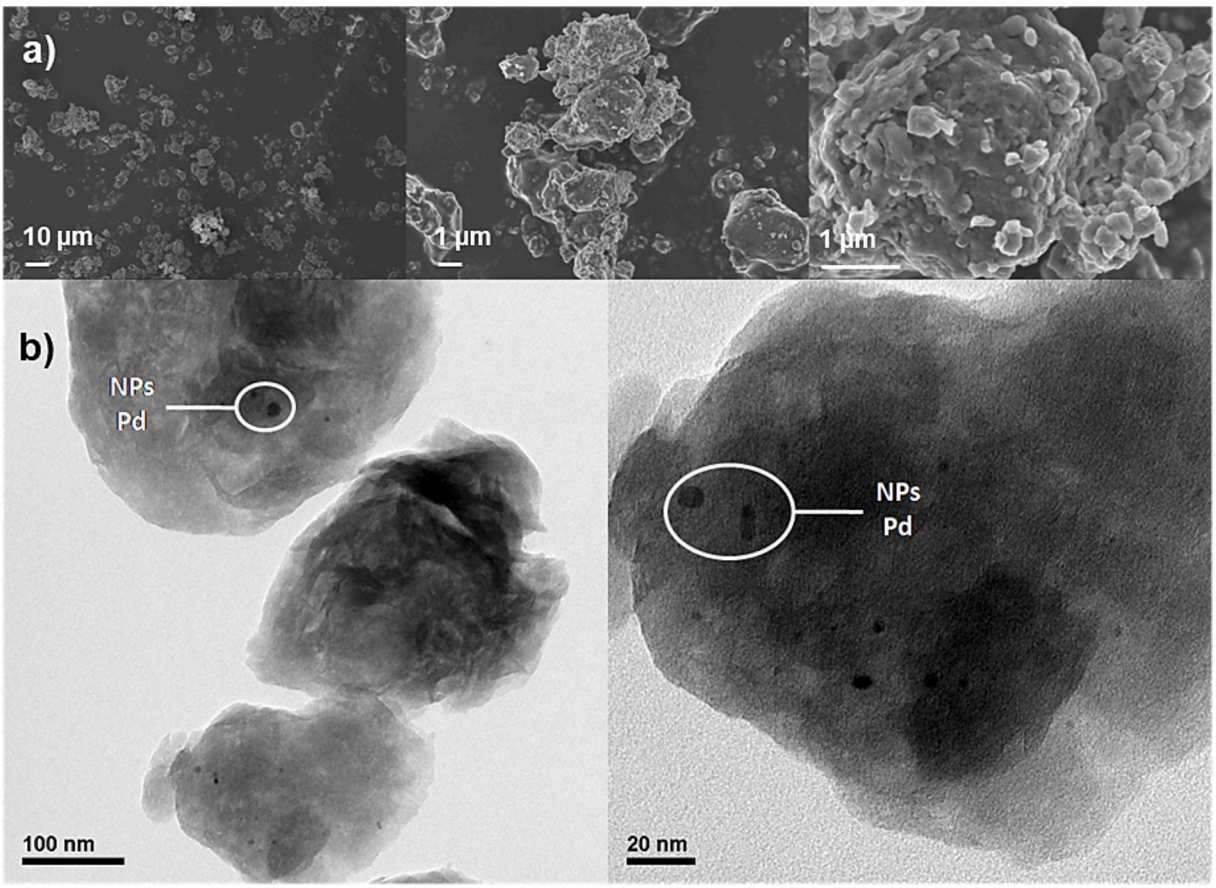

Fig. 2. (a) FESEM and (b) TEM micrographs of the PVP-Pd NPs/laponite® system after 8 cycles of hydrogenation (see Table 2). Magnifications: (650, 5000×, 20,000×, 50,000×).

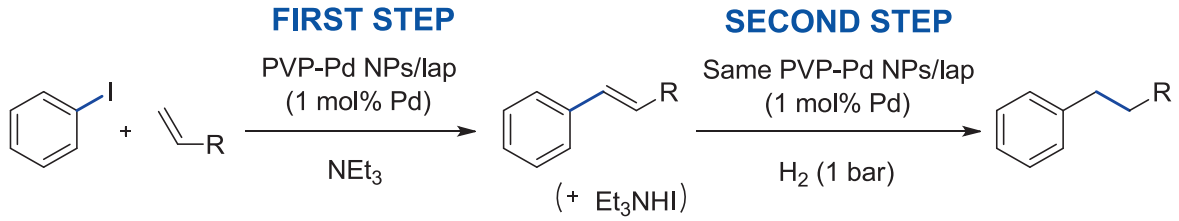

Scheme 3. Heck-Mizoroki C–C coupling plus hydrogenation one-pot reactions catalyzed by the PVP-Pd NPs/laponite® system.

Table 3
Tandem reaction results and catalyst recoverability.

Entry [a]	Substrate	Cycle	Step 1 conv. (%) [b]	Step 2 conv. (%) [b]	Isolated yield (%) [b]	$TON_{(s1)}$/ $TON_{(s2)}$
1	**1**	1	100	100	91	93/91
2	**1**	2	100	0	89	89/0
3	**1**	3	100	0	90	90/0
4	**2**	1	100	89	87	94/87
5	**2**	2	100	0	85	85/0
6	**2**	3	100	0	93	93/0
7[c]	**2**	4	100	0	95	95/0

[a] Reaction conditions: First step: 1 mol% Pd, 100 °C, 3–8 h, NEt_3. Second step: 1 mol% Pd, H_2 (1 bar), 80 °C, 10-15 min. [b] Conversion and selectivity were determined by GC and ^1H NMR. [c] Catalyst calcination before reuse.

catalyze further hydrogenation reactions. To prove this, we eliminated Et_3NHI by calcination in order to evaluate its effect in the catalyst recoverability. Nevertheless, as can be seen in Entry 7 (Table 3, and in the TEM micrographs in Fig. 4), the calcined solid catalyst recovered the activity for the coupling reaction —providing even 95% of isolated yield—, but it was still inactive in hydrogenation.

To sum up, the catalyst used in the hydrogenation of *(E)*-butyl cinnamate (**1**) is still active in both reactions (coupling and hydrogenation), however the catalyst recovered after the coupling reaction losses the activity for hydrogenation, and the formation of triethylammonium iodide does not seem to be responsible for this deactivation.

A plausible explanation for this phenomenon of directional deactivation of the tandem catalyst, only for one of the two studied reactions, relies on their different mechanism. Whereas the Heck-Mizoroki coupling reaction requires the initial formation of Pd(II) active species, hydrogenation reactions are catalyzed by a surface of metallic Pd (0) [24]. Therefore, the progressive formation of Pd(II) over the surface

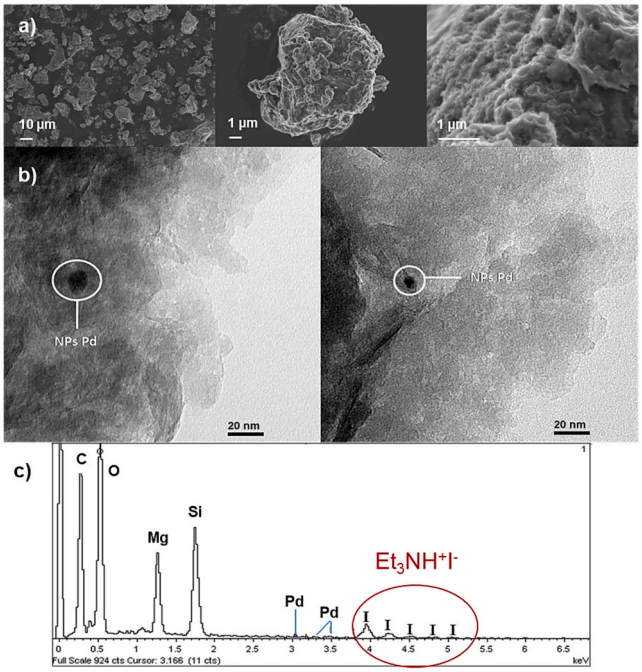

Fig. 3. (a) FESEM images (Magnifications: 650, 5000×, 20,000×), (b) TEM micrographs (Magnification: 50,000×), and c) EDX spectrum of the PVP-Pd NPs/laponite® system after catalyzing the Heck-Mizoroki/hydrogenation coupled process.

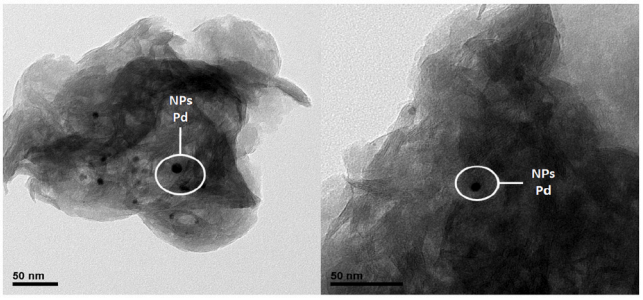

Fig. 4. TEM micrographs of the regenerated PVP-Pd NPs/laponite® system by calcination after catalyzing the coupled process. Magnification: (20,000×).

of the nanoparticles, as a result of their catalytic activity, would trigger the deactivation of the catalyst for subsequent hydrogenations —by decreasing the exposed Pd(0) active surface—, but not for subsequent coupling reactions —which would be even more activated—. This entirely agrees with the experimental results gathered in Table 3. In fact, the results obtained, even in the first reaction, are worse (Table 3, entry 4) than those obtained when the fresh PVP-Pd NPs/laponite® system is used for hydrogenation.

This hypothesis was finally fully confirmed by high-resolution X-ray Photoelectronic Spectroscopy (XPS) analyses of the catalytic systems before and during catalysis. This technique allowed for the characterization of the chemical composition of the Pd nanoparticles surface, which is the catalytic active surface. As detailed in the Experimental Section, different experiments at different speeds (X-ray exposure times) and spectrum regions were carried out in duplicate, in order to avoid possible in situ reduction of palladium during analysis.

Unfortunately, the first XPS analyses revealed that the fundamental Pd 3d region was masked by magnesium from the laponite® clay support. Therefore, a new catalytic system was prepared by supporting the PVP-Pd NPs over silica instead of laponite®. This PVP-Pd NPs/silica

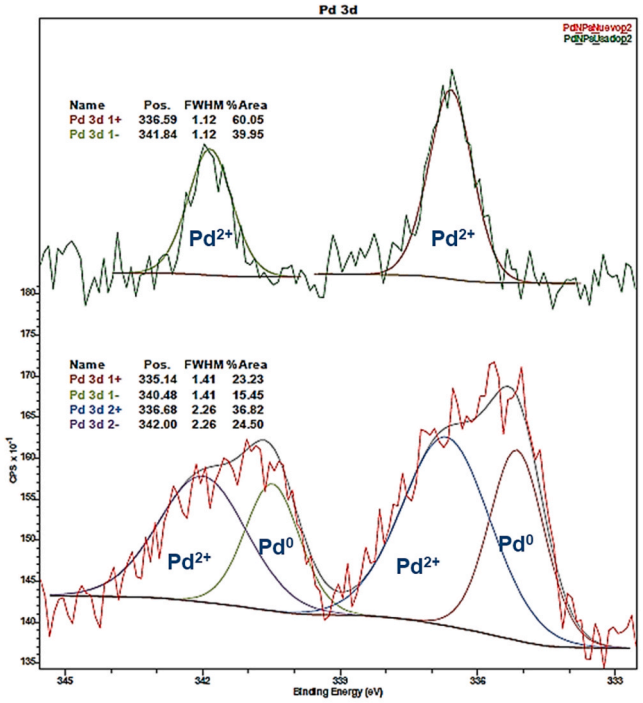

Fig. 5. High Resolution XPS spectrum of supported PVP-Pd NPs at solid state for Pd(0) $3d_{3/2}$ region before (below, in red) and after catalyzing the tandem process (up, in green). (For interpretation of the references to colour in this figure legend, the reader is referred to the web version of this article.)

system was tested in a one-pot process consisting on the Heck-Mizoroki reaction to *n*-butyl cinnamate (**1**) and its subsequent hydrogenation, observing identical catalytic results and deactivation behavior in the case of silica as the results described in Table 3 for laponite®. In this case, XPS spectra for the Pd(0) region were successfully acquired at high resolution for the supported catalytic system before and after catalyzing the tandem process (Fig. 5, below and up, respectively).

The high resolution XPS spectrum shows —see Fig. 5 in red colour—, for the case of the freshly prepared catalyst (before using it in catalysis), two different Pd species, with Pd $3d_{5/2}$ at around 335 eV and 336.5 eV, which are compatible with bulk Pd(0) and with Pd(II) in Pd(0), respectively.[51] In other words, the reducing agent used —ethanol—, which was chosen for its affordability, bio-sourced origin, and, above all, its greater safety compared to other reductants, is not capable of completely reducing all of the Pd(II) present in the precursor to Pd(0) during the synthesis of the Pd NPs; thus, a significant proportion of Pd (II) remains in the freshly prepared NPs. This initial presence of Pd(II) does not limit the resulting catalytic activity at all, rather, in our case it has been shown to be effective in minimizing the preliminary NPs activation for coupling reactions. Furthermore, the ratio of Pd(II) to Pd (0) in the NPs does not seem to change over time, which demonstrates the catalyst's stability.

In the case of the catalysts analyzed after catalyzing the tandem process —see Fig. 5 in green colour—, the Pd 3d region reveals one single palladium species, with Pd $3d_{5/2}$ at around 336.5 eV. These experiments allowed to confirm that the fresh catalyst mainly presents a zero-valent palladium surface, while the used catalyst surface is exclusively composed of Pd(II), therefore inactive for further hydrogenation reactions. Pd(I) species were not identified in any of the XPS experiments conducted.

All of these analyses confirm the formation of Pd(II) on the surface of the catalyst only during coupling reactions, thus these palladium nanoparticles recovered by Pd(II) are active for further C–C coupling reactions but not for further hydrogenations. More importantly, these results are in clear agreement with the proposed release-and-capture

mechanism for the Pd-catalyzed coupling reactions [52,53].

Anyway, after the mechanistic comprehension of the selective deactivation of our catalytic systems towards hydrogenation, in order to reach a further confirmation and, above all, prove that this is not a limitation to the practical use of our systems, we addressed the regeneration of the zero-valent palladium surface. The used catalytic systems —exhibiting Pd(II) surface in the nanoparticles— were treated with simply ethanol under the same conditions required for the synthesis of fresh Pd NPs, *i.e.* stirring the system by heating at 100 °C for 3 h. After this straightforward treatment, the Pd(0) surface was restored to its original state, showing these catalysts quantitative conversions in the hydrogenation of the unsaturated substrates. These as-regenerated systems can be reused for several hydrogenation cycles while preserving their catalytic activity, and even be easily regenerated after catalyzing subsequent coupling reactions.

Finally, supplementary experiments were carried out in selected conventional solvents to compare the catalyst performance with the solventless system. In the case of using toluene as the reaction medium, the PVP-Pd NPs/laponite® catalyst was 3 times less active in the coupling reaction (10 h^{-1} vs. 31 h^{-1} under solvent-free conditions), just achieving 33% conversion of the Heck-Mizoroki substrate (Table S-5). In the case of using ethanol, the catalyst presented similar reactivity than using toluene (42% conversion), but in this case with minimal selectivity towards the desired product (2 h^{-1}). In other words, not only is the catalytic activity reduced when a solvent is used, but in the case of ethanol, iodobenzene is largely hydrodehalogenated to benzene (as identified by GC). Moreover, the Pd leaching determined by ICP-OES in the case of toluene, over 0.5%, is slightly higher than that of the solventless system, whereas in the case of ethanol it is twice as much (*ca.* 1%).

Furthermore, the hydrogenation of the coupling substrate was no possible using both conventional solvents (0% conversion, Table S-6), which demonstrates in this case the impossibility of combining both reactions in a one-pot stepwise approach using conventional solvents, unlike the active solvent-free PVP-Pd NPs/laponite® system.

2.5. Coupled processes for the production of higher-value chemicals

The catalytic PVP-Pd NPs/laponite® system was then applied to the synthesis of a higher-added value chemical, nabumetone, as a proof of concept of its applicability in real coupled processes. Nabumetone (4-(6-methoxynaphtalen-2-yl)butan-2-one) is a non-steroidal anti-inflammatory drug applied in the management of arthritis and rheumatoid diseases to reduce pain and inflammation [54].

In particular, nabumetone was selectively synthesized by a Pd-catalyzed coupled process consisting on a Heck-Mizoroki coupling followed by hydrogenation (Scheme 4). The use of the catalytic system designed in this work allowed the one-pot preparation of this pharmaceutical product with 91% isolated yield. This means that the system is able to promote both coupling plus hydrogenation, remaining afterwards active for coupling reactions but not for hydrogenations, unless being straightforwardly regenerated as described above.

Interestingly, when the synthesis of nabumetone was carried out in a consecutive approach —that implies two sequential reaction steps with isolation of the intermediate between both steps—, the isolated yield only decreased up to 89% (see spectra in section S-3.12).

Secondly, we decided to extend the scope of coupled processes using our catalytic system. Therefore, the designed catalyst was applied to the scalable synthesis of bibenzyl (1,2-diphenylethane) and *(Z)*-stilbene (1,2-diphenylethene) through a Heck-Cassar-Sonogashira coupling plus hydrogenation one-pot stepwise process (Scheme 5). These molecules are produced in large amounts for the synthesis of flame-retardant polymers and antitumor molecules, in the first case, and in the manufacturing of dyes and laser devices, in the second case.

When coupling the Heck-Cassar-Sonogashira (copper-free) reaction, instead of the Heck-Mizoroki coupling, with hydrogenation reactions, the PVP-Pd NPs/laponite® system achieved total conversion of the corresponding substrates in both reaction steps. In this case, the coupling step required a longer reaction time for the selective preparation of the desired product, namely diphenylacetylene. Then, complete hydrogenation of the alkyne to the corresponding alkane (bibenzyl, Scheme 5 up) was achieved in less than 10 s under mild reaction conditions (80 °C, 1 bar), providing a TOF value for the catalyst of *ca.* 35,000 h^{-1}.

The catalytic system resulting after catalyzing a coupling plus hydrogenation cycle was reused to promote a second Heck-Cassar-Sonogashira reaction. As a result, diphenylacetylene was quantitatively obtained. Surprisingly, this partially-deactivated system was then able to carry out the one-pot semihydrogenation of the alkyne to the alkene (the uncommon *(Z)*-stilbene) with 100% of alkyne conversion and 55% of chemoselectivity. In this case, the reaction selectivity is compromised by the complete hydrogenation towards 1,2-diphenylethane. Therefore, fine control of hydrogenation time is essential to obtain the desired product.

3. Experimental section

All reagents and deuterated solvents were purchased as reagent grade from commercial sources (Sigma-Aldrich). Ethanol (99.8%) was purchased from Scharlab. Laponite® RD was obtained from Rockwood Clay Additives GmbH. Silica was purchased from Merck. All manipulations were carried out by using Schlenk techniques under inert atmosphere, unless otherwise stated. Pressure reactions were performed in a Top Industrie Autoclave. Conversions and product yields were determined by Gas Chromatography using Hewlett-Packard 7890 and 6890 Series II chromatographs equipped with a flame ionization detector. All GC details can be found in the Supplementary Information. Reaction products were characterized by NMR using a Bruker Advance 400 MHz spectrometer. Full characterization of all coupling and hydrogenation products is gathered in the Supplementary Information.

3.1. Preparation and characterization of the catalytic systems

A 2 mM H_2PdCl_4 solution was prepared by mixing 35.4 mg of the palladium precursor, $PdCl_2$ (0.2 mmol), 2 mL of 0.2 M HCl, and 98 mL of distilled water. This 2 mM H_2PdCl_4 solution (100 mL) was then mixed in a 500 mL round-bottom flask with 140 mL of distilled water, 94 mL of ethanol, and 444.6 mg of poly-*N*-vinylpyrrolidone (PVP, 10,000 g

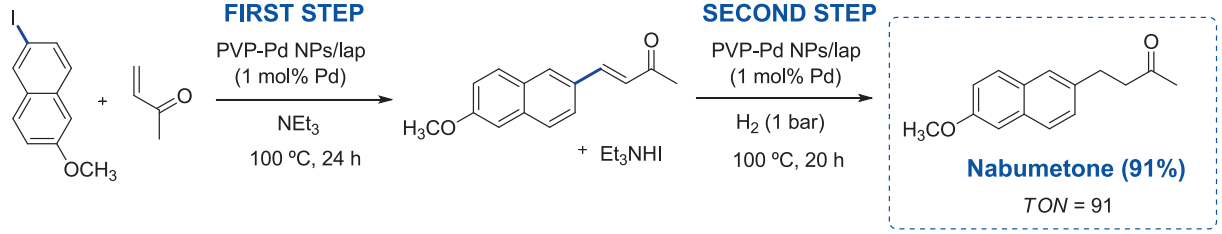

Scheme 4. Synthesis of drug Nabumetone by a Heck-Mizoroki plus hydrogenation coupled process catalyzed by the PVP-Pd NPs/laponite® system.

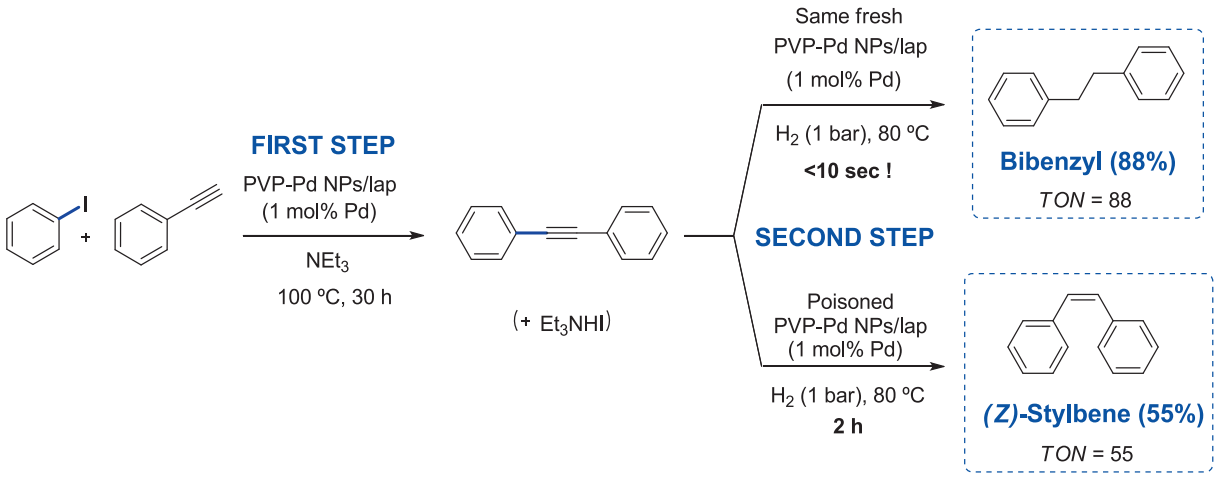

Scheme 5. Heck-Cassar-Sonogashira coupling/hydrogenation coupled process catalyzed by the PVP-Pd NPs/laponite® system.

mol^{-1}), stirring under reflux and inert atmosphere for 3 h. The resulting black dispersion was evaporated at reduced pressure, and washed with absolute ethanol. Finally, the remaining black solid was dissolved in 66 mL of ethanol to form the stable black colloidal solution of PVP-Pd NPs (3 mM) in ethanol. For the preparation of the catalytic systems consisting on PVP-Pd NPs supported over clay, 1 mL of colloidal solution of PVP-Pd NPs (3 mM) in ethanol, 1 g of laponite® clay, and 6 mL of dichloromethane were mixed and magnetically stirred in a 22 mL Schlenk flask for 20 min. Then, both solvents were fully removed under vacuum, resulting a grey solid powder that was kept under inert atmosphere.

Field Emission FESEM micrographs were obtained from a Carl Zeiss MERLIN^{TM} microscope. TEM microscopy analyses were carried out in a JEOL-2000 FXII microscope. X-ray difraction analysis was carried out using an Empyrean diffractometer from PAN analytical (Laboratory of Advanced Microscopy, University of Zaragoza), using X-ray emitted by a copper anode —α wavelength (Cu Kα1, Kα2) = 1.540598 Å and 1.544426 Å—, under a voltage of 45 kV. The BET specific surface was determined by nitrogen physisorption determination at –196 °C using a Micrometrics ASAP 2010 instrument. Pd surface composition was determined by XPS measurements by means of a Kratos AXIS Supra photoelectron spectrometer (Laboratory of Advanced Microscopy, University of Zaragoza) equipped with a monochromated AlKα radiation source ($h\nu$ = 1486.6 eV) and a 280 W electron beam power. The emission of photoelectrons from the sample was analyzed at a takeoff angle of 45° under ultra-high vacuum ($\leq 10^{-9}$ mbar). To identify possible in situ Pd reduction effects during analysis, rapid measurements of the region Pd 3d were initially performed prior to slower analysis in other regions. Binding energies were calibrated against the C 1s (C–C) energy at 284.8 eV, and the element peak intensities were corrected by Scofield factors. The spectra were fitted using Casa XPS 2.1.0.1 version software (Casa Software Ltd, U.K.). Palladium was determined in the catalytic systems and in the extraction supernatants by ICP-OES analyses using a Thermo Scientific i CAP PRO XP Duo spectrometer from the Servicio de Análisis Químico of the University of Zaragoza.

3.2. First step: C–C coupling reaction

The catalytic system (1 mol% Pd) was placed into a 22 mL Schlenk flask. Then, a mixture of 0.3 mmol of iodobenzene (or 1-iodo-3,5-dimethoxybenzene in the case of resveratrol), 0.5 mmol of the corresponding olefin, and 0.75 mmol of triethylamine was deposited and adsorbed onto the solid catalyst. The Schlenk flask was sealed with inert atmosphere and heated at 100 °C using an oil bath. Reaction time varied from 3 h to 24 h, depending on the used alkene. After this time, the reaction product was recovered by extraction with *n*-hexane at 65 °C using vigorous stirring and periods of 15 min between each extraction (1 × 10 mL and 3 × 5 mL). Quantification was carried out by gas chromatography using *n*-decane as an external standard and by ^{1}H NMR after filtration and evaporation. Purification of the products was carried out by silica column chromatography. The solid catalyst was dried in the Schlenk flask under reduced pressure to be ready to be reused in further cycles.

3.3. Second step: hydrogenation reaction

The catalytic system (1% mol Pd) was placed into a 20 mL autoclave vessel and 0.3 mmol of the corresponding unsaturated substrate was adsorbed on it. Then, the air was removed and the system was pressurized with 1 bar of H_2, sealed under inert atmosphere, and finally heated at 80–100 °C and stirred for 10–45 min. After this time, the system was cooled down and the reaction product was recovered by extraction at 65 °C (2 × 10 mL and 2 × 5 mL). Quantification was carried out by gas chromatography using *n*-decane as an external standard and by ^{1}H NMR after filtration and evaporation. The solid catalyst was dried under reduced pressure to be reused in further reaction cycles.

3.4. One-pot reactions general procedure

The catalytic system (1 mol% Pd) was placed into a 20 mL autoclave vessel. Then, the reaction mixture (0.3 mmol of iodobenzene, 0.5 mmol of olefin, and 0.75 mmol of triethylamine) was added to be adsorbed onto the solid catalyst. The system was sealed under inert atmosphere and heated at 100 °C using an oil bath for 3–20 h. After this time, the system was cooled down and the argon was removed under reduced pressure prior to its pressurization with 1 bar of H_2. Then, the vessel was heated at 80–100 °C until total conversion. Finally, the system was cooled down and the reaction product was recovered by extraction with *n*-hexane at 65 °C (2 × 10 mL and 2 × 5 mL). Quantification was carried out by gas chromatography using *n*-decane as the standard and by ^{1}H NMR (after filtration and evaporation). The solid catalyst was dried under vacuum prior to be ready for reuse.

3.5. One-pot synthesis of nabumetone

The above designed catalytic system (1 mol% Pd) was placed into a 20 mL autoclave vessel, together with the reaction mixture (0.3 mmol of 2-iodo-6-methoxynaphtalene, 2.01 mmol of but-3-en-2-one, and 2.17 mmol of triethylamine). Then, this system was sealed under inert atmosphere and kept at 100 °C for 24 h. After this time, the vessel was cooled down to room temperature and put under reduced pressure prior to its pressurization with 1 bar of H_2. The system was heated at 100 °C for 20 h. Finally, the system was cooled down to room temperature and

the final reaction product (nabumetone) was recovered by extraction with dichloromethane (2 × 10 mL and 2 × 5 mL). Quantification (91% isolated yield) was carried out by ^{1}H NMR after elimination of the extraction solvent under reduced pressure and purification by Combiflash® silica gel column chromatography (hexane-DCM 95:5 with elution gradient to 0:100).

3.6. Heck-Cassar-Sonogashira coupling/hydrogenation coupled process

The catalytic system (1 mol% Pd) was placed into a 20 mL autoclave vessel, together with the reaction mixture (0.3 mmol of iodobenzene, 0.3 mmol of phenylacetylene, and 0.75 mmol of triethylamine). Afterwards, the autoclave vessel was sealed under inert atmosphere, kept at 100 °C for 30 h, cooled down to room temperature, and repressurized with 1 bar of H_2. The system was then heated at 80 °C for 10 sec, and finally cooled down to carry out the product (bibenzyl) extraction with *n*-hexane (2 × 10 mL and 2 × 5 mL). Quantification (88% isolated yield) was carried out by ^{1}H NMR after elimination of solvents under reduced pressure and purification by silica gel column chromatography (hexane-DCM).

4. Conclusions

In this work, we present an active, selective, recoverable, and regenerable catalytic system based on Pd nanoparticles supported over affordable clay laponite® to promote one-pot stepwise and consecutive reactions with, a priori, incompatible mechanisms, under solvent-less conditions. The designer solid catalyst is able to catalyze over 50 reaction cycles of the Heck-Mizoroki coupling between iodobenzene and differently-substituted acrylates and styrenes, as well as the Heck-Cassar-Sonogashira reaction of iodobenzene with phenylacetylene, the hydrogenation of a large scope of olefins and alkynes within short time (up to 10 s) under mild conditions, and all their coupled combinations (consecutive one-pot hydrogenations). As proof-of-concepts of the catalyst applicability, the synthesis of commercial drugs resveratrol and nabumetone was achieved using the PVP-Pd NPs/laponite® systems, with isolated yields over 90%.

After catalyzing a coupled coupling reaction plus hydrogenation process, the designer catalytic system is still able to perform multiple further coupling reactions without apparent deactivation. The formation of triethylammonium iodide salt has been proven to have scarce influence on the catalyst recoverability, in any case it can be eliminated by calcination. Interestingly, we discovered that the afore described used catalytic system is not able to catalyze hydrogenation reactions, due to the oxidation of the Pd NP surface from Pd(0) to Pd(II), unless a reversible and straightforward regeneration of the catalyst with ethanol as a reductant is carried out. This deactivation behavior, only towards hydrogenation, after catalyzing coupling reactions, allowed us to confirm by high resolution XPS analyses the “release and capture” mechanism for the coupling reactions catalyzed by Pd NPs, while hydrogenation requires a zero-valent palladium surface to occur.

Funding Sources

Agencia Estatal de Investigación of Spain (PID2021-125762NB-I00) and Gobierno de Aragón (E37_23R).

CRediT authorship contribution statement

Jorge Cambronero-Arregui: Writing – review & editing, Methodology, Investigation. **Alejandro V. Martínez:** Writing – review & editing, Methodology, Investigation, Data curation. **Elisabet Pires:** Writing – review & editing, Funding acquisition. **José A. Mayoral:** Writing – review & editing, Supervision, Funding acquisition, Conceptualization. **Alejandro Leal-Duaso:** Writing – review & editing, Writing – original draft, Supervision, Methodology, Investigation, Funding acquisition, Data curation, Conceptualization.

Declaration of competing interest

The authors declare that they have no known competing financial interests or personal relationships that could have appeared to influence the work reported in this paper.

Acknowledgements

This investigation was developed within the scope of the projects PID2021-125762NB-I00 from Agencia Estatal de Investigación (AEI) of Spain and the Research Group E37_23R from the Gobierno de Aragón. A. C. Gallego, from the Service of Electron Microscopy of Materials of the University of Zaragoza is acknowledged for her assistance in the FESEM and TEM experiments. G. Antorrena, from the Laboratory of Advanced Microscopy (LMA) of the University of Zaragoza is sincerely thanked for his valuable assistance in XPS and XRD analyses. The Servicio de Análisis Químico of the University of Zaragoza is acknowledged for helping with the ICP analyses.

Appendix A. Supplementary data

The list of abbreviations (Glossary), the gas chromatography analysis details, the complete characterization of all coupling and hydrogenation products, additional characterization information of catalytic systems, and detailed information on additional experiments can be found in the Electronic Supplementary Information. Supplementary data to this article can be found online at https://doi.org/10.1016/j.jcat.2026.116860.

Data availability

Data will be made available on request.

References

[1] N. Joudeh, A. Saragliadis, G. Koster, P. Mikheenko, D. Linke, Synthesis methods and applications of palladium nanoparticles: a review, Front. Nanotechnol. 4 (2022) 1062608–1062631, https://doi.org/10.3389/fnano.2022.1062608.
[2] A. Bej, K. Ghosh, A. Sarkar, D.W. Knight, Palladium nanoparticles in the catalysis of coupling reactions, RSC Adv. 6 (2016) 11446–11453, https://doi.org/10.1039/C5RA26304B.
[3] A. Reina, A. Serrano-Maldonado, E. Teuma, E. Martin, M. Gómez, Palladium nanocatalysts in glycerol: tuning the reactivity by effect of the stabilizer, Catal. Commun. 104 (2018) 22–27, https://doi.org/10.1016/j.catcom.2017.10.004.
[4] T. Maxson, T. Szilvási, Metal-support interactions reshape nanoparticle catalyst surfaces, Angew. Chem. 1 (2025) e70008, https://doi.org/10.1002/anov.70008.
[5] I. Ijaz, E. Gilani, A. Nazir, A. Bukhari, Detail review on chemical, physical and green synthesis, classification, characterizations and applications of nanoparticles, Green Chem. Lett. Rev. 13 (2020) 59–81, https://doi.org/10.1080/17518253.2020.1802517.
[6] A. Leal-Duaso, J.A. Mayoral, E. Pires, Steps forward toward the substitution of conventional solvents in the Heck–Mizoroki coupling reaction: glycerol-derived ethers and deep eutectic solvents as reaction media, ACS Sust. Chem. Eng. 8 (2020) 13076–13084, https://doi.org/10.1021/acssuschemeng.0c04862.
[7] D. Astruc, Palladium nanoparticles as efficient green homogeneous and heterogeneous carbon−carbon coupling precatalysts: a unifying view, Inorg. Chem. 46 (2007) 1884–1894, https://doi.org/10.1021/ic062183h.
[8] M.R. Bailey, T.A. Gmür, F. Grillo, L. Isa, Modular attachment of nanoparticles on microparticle supports via multifunctional polymers, Chem. Mater. 35 (2023) 3731–3741, https://doi.org/10.1021/acs.chemmater.3c00555.
[9] T.M. Eggenhuisen, P.E. de Jongh, Supported Metal Nanoparticles, in: C. De Mello Donega (Ed.), Nanoparticles: Workhorses of Nanoscience, Springer Nature Switzerland, Cham, 2024, pp. 131–150. 10.1007/978-3-031-71460-3_5.
[10] A.V. Martínez, A. Leal-Duaso, J.I. García, J.A. Mayoral, An extremely highly recoverable clay-supported Pd nanoparticle catalyst for solvent-free Heck–Mizoroki reactions, RSC Adv. 5 (2015) 59983–59990, https://doi.org/10.1039/C5RA10191C.
[11] A.V. Martínez, F. Invernizzi, A. Leal-Duaso, J.A. Mayoral, J.I. García, Microwave-promoted solventless Mizoroki–Heck reactions catalysed by Pd nanoparticles supported on laponite clay, RSC Adv. 5 (2015) 10102–10109, https://doi.org/10.1039/C4RA15418E.

[12] I. Fatimah, G. Fadillah, I. Yanti, R. Doong, Clay-supported metal oxide nanoparticles in catalytic advanced oxidation processes: a review, Nanomat 12 (2022) 825–858, https://doi.org/10.3390/nano12050825.

[13] L.-C. Campeau, N. Hazari, Cross-coupling and related reactions: connecting past success to the development of new reactions for the future, Organometallics 38 (2019) 3–35, https://doi.org/10.1021/acs.organomet.8b00720.

[14] A. Clemente, J. Cambronero-Arregui, J.A. Aínsa, E. Pires, J.A. Mayoral, A. Leal-Duaso, Bio-based functional ionic liquids for a novel approach to Sonogashira coupling in the absence of copper and external bases, ACS Sust. Chem. Eng. (2026), https://doi.org/10.1021/acssuschemeng.6c00237.

[15] Y. Song, S. Liu, P. Sun, W. Qiu, Y. Li, C. Peng, Catalytic and engineering strategies for enhanced hydrogenation reactions: a review of heterogeneous catalysts and process optimization, Res. Eng. 25 (2025) 103958–103975, https://doi.org/10.1016/j.rineng.2025.103958.

[16] A. Leal-Duaso, J.M. Fraile, Chloroaromatics remediation: insights into the chemical reduction and hydrodechlorination of chlorobenzenes, Crit. Rev. Environ. Sci. Technol. 55 (2025) 1628–1656, https://doi.org/10.1080/10643389.2025.2560432.

[17] A. Leal-Duaso, L. Salvatella, J.M. Fraile, Physical-chemical transformations for the remediation and valorization of hexachlorocyclohexanes (HCHs) including lindane: a review, J. Environ. Manage. 375 (2025) 124262–124300, https://doi.org/10.1016/j.jenvman.2025.124262.

[18] A. Leal-Duaso, I. Favier, D. Pla, E. Pires, M. Gómez, Design of glycerol-based solvents for the immobilization of palladium nanocatalysts: a hydrogenation study, ACS Sust. Chem. Eng. 9 (2021) 6875–6885, https://doi.org/10.1021/acssuschemeng.1c01694.

[19] S.D. Roughley, A.M. Jordan, The medicinal chemist's toolbox: an analysis of reactions used in the pursuit of drug candidates, J. Med. Chem. 54 (2011) 3451–3479, https://doi.org/10.1021/jm200187y.

[20] S. Nishimura, Handbook of Heterogeneous Catalytic Hydrogenation for Organic Synthesis, Wiley-VCH, New York, 2001. 2025,, 10.1021/op0100798 (Accessed October 1).

[21] A.P. Umpierre, G. Machado, G.H. Fecher, J. Morais, J. Dupont, Selective hydrogenation of 1,3-butadiene to 1-butene by Pd(0) nanoparticles embedded in imidazolium ionic liquids, Adv. Synth. Catal. 347 (2005) 1404–1412, https://doi.org/10.1002/adsc.200404313.

[22] N. Semagina, L. Kiwi-Minsker, Palladium nanohexagons and nanospheres in selective alkyne hydrogenation, Catal. Lett. 127 (2009) 334–338, https://doi.org/10.1007/s10562-008-9684-1.

[23] Y.-M. Lu, H.-Z. Zhu, W.-G. Li, B. Hu, S.-H. Yu, Size-controllable palladium nanoparticles immobilized on carbon nanospheres for nitroaromatic hydrogenation, J. Mater. Chem. A 1 (2013) 3783–3788, https://doi.org/10.1039/c3ta00159h.

[24] R. Sablong, U. Schlotterbeck, D. Vogt;, S. Mecking, Catalysis with soluble hybrids of highly branched macromolecules with palladium nanoparticles in a continuously operated membrane reactor, Adv. Synth. Catal. 345 (2003) 333–336, https://doi.org/10.1002/adsc.200390034.

[25] O.M. Wilson, M.R. Knecht, J.C. Garcia-Martinez, R.M. Crooks, Effect of Pd nanoparticle size on the catalytic hydrogenation of allyl alcohol, J. Am. Chem. Soc. 128 (2006) 4510–4511, https://doi.org/10.1021/ja058217m.

[26] A.P. Alonso, S. Mauriés, J.-B. Ledeuil, L. Madec, D.P. Minh, D. Pla, M. Gómez, Nickel nanoparticles immobilized on pristine halloysite: an outstanding catalyst for hydrogenation processes, ChemCatChem 14 (2022) e202200775, https://doi.org/10.1002/cctc.202200775.

[27] J. Kou, W.D. Wang, J. Fang, F. Li, H. Zhao, J. Li, H. Zhu, B. Li, Z. Dong, Precisely controlled Pd nanoclusters confined in porous organic cages for size-dependent catalytic hydrogenation, Appl. Catal. B Environ. 315 (2022) 121487–121498, https://doi.org/10.1016/j.apcatb.2022.121487.

[28] Q. Song, W. David Wang, K. Lu, F. Li, B. Wang, L. Sun, J. Ma, H. Zhu, B. Li, Z. Dong, Three-dimensional hydrophobic porous organic polymers confined Pd nanoclusters for phase-transfer catalytic hydrogenation of nitroarenes in water, Chem. Eng. J. 415 (2021) 128856–128867, https://doi.org/10.1016/j.cej.2021.128856.

[29] H. Zhao, C. Liu, Y. Zheng, S. Li, Y. Gao, Q. Ma, F. Wang, Z. Dong, Precisely designed nitrogen-doped mesoporous carbon sphere-confined electron-deficient Pd nanoclusters with enhanced catalytic hydrogenation performance, ACS Catal. 14 (2024) 8619–8630, https://doi.org/10.1021/acscatal.4c02348.

[30] Q. Ma, J. Cheng, X. Wu, J. Xie, R. Zhang, Z. Mao, H. Yang, W. Fan, J. Zeng, J. H. Bitter, G. Li, Z. Li, C. Li, C–C bond coupling with sp3 C–H bond via active intermediates from CO_2 hydrogenation, Nat. Commun. 16 (2025) 140–151, https://doi.org/10.1038/s41467-024-55640-w.

[31] M.H.K. Lee, H. Yin, W.U. Khan, F.L.Y. Lam, Y. Ok, M.J. Watson, S. Pang, A.C.K. Yip, A new hydrogenation-coupling approach for supra-equilibrium conversion in a water–gas shift reaction: simultaneous hydrogen generation and chemical storage, Int. J. Hydr. Energ. 48 (2023) 18567–18571, https://doi.org/10.1016/j.ijhydene.2023.02.019.

[32] A. Leal-Duaso, S. Gracia-Barberán, J.A. Mayoral, J.I. García, E. Pires, Readily scalable methodology for the synthesis of nonsymmetric glyceryl diethers by a tandem acid-/base-catalyzed process, Org. Process Res. Dev. 24 (2020) 154–162, https://doi.org/10.1021/acs.oprd.9b00411.

[33] Z. Chen, S. Yang, J. Yang, B. Zhang, H. Jiang, R. Gao, T. Wang, Q. Zhang, H. Zhang, Boosting catalytic hydrogen transfer cascade reactions via tandem catalyst design by coupling co single atoms with adjacent co clusters, ACS Catal. 14 (2024) 18256–18267, https://doi.org/10.1021/acscatal.4c05569.

[34] M. Szlosek-Pinaud, P. Diaz, J. Martinez, F. Lamaty, Efficient synthetic approach to heterocycles possessing the 3,3-disubstituted-2,3-dihydrobenzofuran skeleton via diverse palladium-catalyzed tandem reactions, Tetrahedron 63 (2007) 3340–3349, https://doi.org/10.1016/j.tet.2007.02.035.

[35] A. Trejos, L.R. Odell, M. Larhed, Development of stereocontrolled palladium(II)-catalyzed domino heck/suzuki β,α-diarylation reactions with chelating vinyl ethers and arylboronic acids, Chem. Open 1 (2012) 49–56, https://doi.org/10.1002/open.201100010.

[36] Y. Hu, J. Zhou, X. Long, J. Han, C. Zhu, Y. Pan, Palladium-catalyzed cascade reactions of benzyl halides with *N*-allyl-*N*-(2-butenyl)-*p*-toluenesulfonamide, Tetrahedron Lett. 44 (2003) 5009–5010, https://doi.org/10.1016/S0040-4039(03)01177-8.

[37] J. Hitce, O. Baudoin, Substituted benzocarbocycles by palladium-catalyzed cascade reactions featuring a C(sp^3)-H activation step, Adv. Synth. Catal. 349 (2007) 2054–2060, https://doi.org/10.1002/adsc.200700099.

[38] R.T. Ruck, M.A. Huffman, M.M. Kim, M. Shevlin, W.V. Kandur, I.W. Davies, Palladium-catalyzed tandem heck reaction/C-H functionalization—preparation of spiro-indane-oxindoles, Angew. Chem. Int. Ed. 47 (2008) 4711–4714, https://doi.org/10.1002/anie.200800549.

[39] V.K. Aggarwal, P.W. Davies, W.O. Moss, A palladium catalysed cyclisation–carbonylation of bromodienes: control in carbonylation over facile β-hydride elimination, Chem. Commun. (2002) 972–973, https://doi.org/10.1039/B201311H.

[40] R. Grigg, S.P. Mutton, Pd-catalysed carbonylations: versatile technology for discovery and process chemists, Tetrahedron 66 (2010) 5515–5548, https://doi.org/10.1016/j.tet.2010.03.090.

[41] Y. Zhao, R. Jin, Y. Chou, Y. Li, J. Lin, G. Liu, Asymmetric transfer hydrogenation–Sonogashira coupling one-pot enantioselective tandem reaction catalysed by Pd(0)–Ru(III)/diamine-bifunctionalized periodic mesoporous organosilica, RSC Adv. 7 (2017) 22592–22598, https://doi.org/10.1039/C7RA03029K.

[42] P. Singh, S. Mishra, A. Sahoo, S. Patra, A magnetically retrievable mixed-valent Fe_3O_4@SiO_2/Pd0/PdII nanocomposite exhibiting facile tandem Suzuki coupling/transfer hydrogenation reaction, Sci. Rep. 11 (2021) 9305–9315, https://doi.org/10.1038/s41598-021-88528-6.

[43] J.R. Patel, A.U. Patel, Pd single-atom-site stabilized by supported phosphomolybdic acid: design, characterizations and tandem Suzuki–Miyaura cross coupling/nitro hydrogenation reaction, Nanoscale Adv. 4 (2022) 4321–4334, https://doi.org/10.1039/D2NA00559J.

[44] K. Geoghegan, S. Kelleher, P. Evans, An investigation into the one-pot Heck olefination-hydrogenation reaction, J. Org. Chem. 76 (2011) 2187–2194, https://doi.org/10.1021/jo200023r.

[45] X. Fan, M.G. Manchon, K. Wilson, S. Tennison, A. Kozynchenko, A.A. Lapkin, P. K. Plucinski, Coupling of Heck and hydrogenation reactions in a continuous compact reactor, J. Catal. 267 (2009) 114–120, https://doi.org/10.1016/j.jcat.2009.07.019.

[46] M. Gruber, S. Chouzier, K. Koehler, L. Djakovitch, Palladium on activated carbon: a valuable heterogeneous catalyst for one-pot multi-step synthesis, Appl. Catal. A-Gen. 265 (2004) 161–169, https://doi.org/10.1016/j.apcata.2004.01.012.

[47] J.-P. Leclerc, M. André, K. Fagnou, Heck, Direct arylation, and hydrogenation: two or three sequential reactions from a single catalyst, J. Org. Chem. 71 (2006) 1711–1714, https://doi.org/10.1021/jo0523619.

[48] M.J. Climent, A. Corma, S. Iborra, M. Mifsud, Heterogeneous palladium catalysts for a new one-pot chemical route in the synthesis of fragrances based on the heck reaction, Adv. Synth. Catal. 349 (2007) 1949–1954, https://doi.org/10.1002/adsc.200700026.

[49] F.-X. Felpin, J. Coste, C. Zakri, E. Fouquet, Preparation of 2-quinolones by sequential Heck reduction-cyclization (HRC) reactions by using a multitask palladium catalyst, Chem. Eur. J. 15 (2009) 7238–7245, https://doi.org/10.1002/chem.200900583.

[50] J.M. Fraile, R. Mallada, J.A. Mayoral, M. Menéndez, L. Roldán, Shift of multiple incompatible equilibriums by a combination of heterogeneous catalysis and membranes, Chem Eur J 16 (2010) 3296–3299, https://doi.org/10.1002/chem.200902759.

[51] A.V. Naumkin, A. Kraut-Vass, S.W. Gaarenstroom, C.J. Powell, NIST Database of Pd (3d5/2) Binding Energies, U.S. Secretary of Commerce on behalf of the United States of America, 2012 https://xpsdatabase.net/palladium-pd-z46-palladiumcompounds.

[52] S. Reimann, J. Stötzel, R. Frahm, W. Kleist, J.-D. Grunwaldt, A. Baiker, Identification of the active species generated from supported Pd catalysts in heck reactions: an in situ quick scanning EXAFS investigation, J. Am. Chem. Soc. 133 (2011) 3921–3930, https://doi.org/10.1021/ja108636u.

[53] C. Pavia, F. Giacalone, L.A. Bivona, A.M.P. Salvo, C. Petrucci, G. Strappaveccia, L. Vaccaro, C. Aprile, M. Gruttadauria, Evidences of release and catch mechanism in the Heck reaction catalyzed by palladium immobilized on highly cross-linked-supported imidazolium salts, J. Mol. Catal. A 387 (2014) 57–62, https://doi.org/10.1016/j.molcata.2014.02.025.

[54] Y. Guo, H. Lee, H. Jeong, Chapter three - gut microbiota in reductive drug metabolism, in: J. Sun (Ed.), Progress in Molecular Biology and Translational Science, Academic Press, 2020, pp. 61–93, https://doi.org/10.1016/bs.pmbts.2020.04.002.